

## Theory of Electron Diffusion Parallel to Electric Fields. II. Application to Real Gases

John J. Lowke and James H. Parker, Jr.

*Westinghouse Research Laboratories, Pittsburgh, Pennsylvania 15235*

(Received 2 December 1968)

The theoretical analysis of the preceding paper is extended to include inelastic collisions. The resulting theory is then used to obtain values for the diffusion coefficient  $D_L$ , which is appropriate for electrons diffusing parallel to an electric field. Theoretical values of  $D_L/\mu$  are compared with values of  $D_T/\mu$  as a function of  $E/N$  for the gases helium, argon, hydrogen, deuterium, nitrogen, oxygen, carbon dioxide, water vapor, carbon monoxide, krypton, and xenon;  $\mu$  is the electron mobility,  $D_T$  is the diffusion coefficient for electron diffusion perpendicular to the electric field,  $E$  is the electric field strength, and  $N$  the number density of the gas. A comparison is also made between theoretical values of  $D_L/\mu$  and the available experimental values of this quantity. Experimental differences that have been observed between  $D_L$  and  $D_T$  of the order of a factor of seven in argon and a factor of two in helium, hydrogen, and nitrogen are satisfactorily explained.

### I. INTRODUCTION

In the preceding paper,<sup>1</sup> hereafter referred to as I, a solution of the Boltzmann equation was obtained which described the diffusion and drift of an electron pulse in a uniform electric field. This solution leads to an expression for the diffusion coefficient  $D_L$ , appropriate to diffusion parallel to the electric field for electrons undergoing only elastic collisions. It was shown that  $D_L$  differs significantly from  $D_T$ , the diffusion coefficient perpendicular to the electric field, when account is taken of the variation of the electron energy distribution with position within the pulse.

In Sec. II of the present paper the theoretical expressions of I are generalized to include inelastic collisions. The method of obtaining numerical values for  $D_L/\mu$  is discussed in Sec. III. Theoretical results are given in Sec. IV for  $D_L/\mu$  and  $D_T/\mu$  as a function of  $E/N$  for the gases helium, argon, hydrogen, deuterium, nitrogen, oxygen, carbon dioxide, water vapor, carbon monoxide, krypton, and xenon. In deriving these quantities, use is made of previously published values of elastic and inelastic cross sections as a function of energy. A comparison is also made between the theoretical values of  $D_L/\mu$  and the available experimental values of this quantity. The accuracy of the computations is discussed in Sec. V.

### III. METHOD OF NUMERICAL SOLUTION

With the inelastic terms included in Eq. (23) of I, which is in  $F_0$ , the equation becomes identical to Eq. (1) of (FP) and can therefore be solved by using their method. Equations (24) and (25), which are in  $F_1$  and  $F_2$ , are identical to the equation in  $F_0$  with the exception of additional terms in  $F_0$  and  $F_1$ . As a consequence it is possible to use the method of (FP) to obtain in turn  $F_0$ ,  $F_1$ , and  $F_2$  from Eqs. (23)–(25) of I.  $F_0$ ,  $F_1$ , and  $F_2$  are the first three terms of an expansion of the distribution function as defined by Eq. (21) of I.

### II. INELASTIC COLLISIONS

In order to evaluate  $D_L/\mu$  for the molecular gases, it is necessary to include the effect of inelastic collisions in the theoretical analysis. Following the treatment of Frost and Phelps,<sup>2,3</sup> subsequently referred to as (FP), the following extra terms are introduced into the right-hand side of the Boltzmann equation in  $f^0$ , as given by Eq. (17) of I,

$$\begin{aligned} & (8\pi/m^2) \left[ \sum_j (\epsilon + \epsilon_j) f^0(\epsilon + \epsilon_j) N Q_j (\epsilon + \epsilon_j) \right. \\ & \quad - \epsilon f^0(\epsilon) N \sum_j Q_j(\epsilon) \\ & \quad + \sum_j (\epsilon - \epsilon_j) f^0(\epsilon - \epsilon_j) N Q_{-j}(\epsilon - \epsilon_j) \\ & \quad \left. - \epsilon f^0(\epsilon) N \sum_j Q_{-j}(\epsilon) \right]. \end{aligned} \quad (1)$$

The first term in Eq. (1) represents electrons of energy  $\epsilon + \epsilon_j$  losing energy  $\epsilon_j$  in an inelastic collision with a cross section  $Q_j$ , while the second term represents electrons of energy  $\epsilon$  losing energy  $\epsilon_j$ . The third and fourth terms correspond to the electrons gaining energy  $\epsilon_j$  due to collisions of the second kind, with a cross section  $Q_{-j}$ . Terms of this type will also appear on the left-hand side of Eqs. (19), (23), (24), and (25) of Paper I. In Eq. (1),  $f^0$  is, of course, a function of  $z$  and  $t$  in addition to the energy.

It is convenient to transform Eqs. (23)–(25) of I to forms similar to those in (FP) by making the substitutions

$$\xi = \epsilon/kT, \quad \theta = Q_m/Q_0, \quad \alpha = (M/6m)(eE/NQ_0kT)^2, \quad \eta_{\pm j} = MQ_{\pm j}/2mQ_0.$$

The equations in  $F_0$ ,  $F_1$ , and  $F_2$ , including the inelastic terms, then become

$$\frac{\partial}{\partial \xi} \left[ \xi^2 \theta F_0 + \xi \left( \frac{\alpha}{\theta} + \xi \theta \right) \frac{\partial F_0}{\partial \xi} \right] + I_0 = 0, \quad (2)$$

$$\frac{\partial}{\partial \xi} \left[ \xi^2 \theta F_1 + \xi \left( \frac{\alpha}{\theta} + \xi \theta \right) \frac{\partial F_1}{\partial \xi} \right] + I_1 + \frac{kT}{eE} \alpha \left[ \frac{\partial}{\partial \xi} \left( \frac{\xi F_0}{\theta} \right) + \frac{\xi}{\theta} \frac{\partial F_0}{\partial \xi} \right] + W \frac{M}{4NQ_0} \left( \frac{2\xi}{mkT} \right)^{\frac{1}{2}} F_0 = 0, \quad (3)$$

and

$$\begin{aligned} \frac{\partial}{\partial \xi} \left[ \xi^2 \theta F_2 + \xi \left( \frac{\alpha}{\theta} + \xi \theta \right) \frac{\partial F_2}{\partial \xi} \right] + I_2 + \frac{kT\alpha}{eE} \left[ \frac{\partial}{\partial \xi} \left( \frac{\xi F_1}{\theta} \right) + \frac{\xi}{\theta} \frac{\partial F_1}{\partial \xi} \right] + (WF_1 - D_L F_0) \frac{M}{4NQ_0} \left( \frac{2\xi}{mkT} \right)^{\frac{1}{2}} \\ + \left( \frac{kT}{eE} \right)^2 \frac{\alpha}{\theta} F_0 \xi = 0, \end{aligned} \quad (4)$$

where  $I_n = \sum_j \xi \eta_j (\xi) [F_n(\xi) - \exp(-\xi_j) F_n(\xi - \xi_j)]$ .

As in (FP), use has been made of the Klein-Rosseland relation. In these equations  $E$  is the electric field,  $k$  is Boltzmann's constant,  $T$  the gas temperature in °K,  $M$  the mass of the gas molecule,  $m$  the electron mass,  $e$  the electron charge,  $W$  (or  $\mu E$ ) the drift velocity,  $Q_m$  the momentum transfer cross section, which is a function of energy,  $Q_{+j}$  the  $j$ th inelastic cross section for energy loss  $kT\xi_j$ ,  $Q_{-j}$  the  $j$ th inelastic cross section for energy gain  $kT\xi_j$ , and  $Q_0$  a reference cross section, which in the present calculation is taken as  $10^{-16}$  cm<sup>2</sup>. The quantities  $Q_{\pm j}$  are functions of energy and include a factor for fractional population of the initial molecular state so that multiplication by the total number density of the gas  $N$  gives the reciprocal of the mean free path for the process.

When Eq. (3) is integrated with respect to  $\xi$  from zero to infinity, one obtains the expression for the drift velocity which is analogous to Eq. (5) of (FP), i. e.,

$$W = \mu E = - (8\pi eEkT/3m^2NQ_0) \int_0^\infty (\xi/\theta) (\partial F_0/\partial \xi) d\xi. \quad (5)$$

In obtaining this relation use is made of the fact that the functions  $F_0$  and  $F_1$  tend to zero at high energy, that the integral over the terms representing inelastic processes is zero due to particle conservation in inelastic collisions and  $F_0$  is normalized<sup>4</sup> as in I by

$$(4\pi kT/m)(2kT/m)^{1/2} \int_0^\infty \xi^{1/2} F_0 d\xi = 1. \quad (6)$$

Equation (5) is identical to Eq. (26) of I except  $\epsilon$  has been expressed in terms of  $\xi$ .

In a similar way, by making use of the requirement that  $F_2$  tends to zero at high energy, integrating Eq. (4) from zero to infinity and dividing by  $\mu$ , we obtain,

$$\frac{D_L}{\mu} = \frac{D_T}{\mu} + \frac{8\pi eEkT}{3m^2\mu NQ_0} \int_0^\infty \frac{\xi}{\theta} \frac{\partial F_1}{\partial \xi} d\xi + \frac{4\pi eEkT}{m} \left( \frac{2kT}{m} \right)^{\frac{1}{2}} \int_0^\infty \xi^{1/2} F_1 d\xi. \quad (7)$$

The ratio  $D_T/\mu$  is given by

$$D_T/\mu = (8\pi/3NQ_0\mu)(kT/m)^2 \int_0^\infty (\xi F_0/\theta) d\xi, \quad (8)$$

where  $D_T$  is given by Eq. (6) of I.

It is convenient to represent the diffusion coefficients  $D_L$  and  $D_T$  by the ratios  $D_T/\mu$  and  $D_L/\mu$ , first because these ratios are functions of  $E/N$  and are pressure independent, and second because in both cases the experimentally observed quantities are not  $D_T$  and  $D_L$ , but  $D_T/\mu$  and  $D_L/\mu$ .

Rather than integrate Eqs. (2)–(4) from 0 to  $\xi$ , in the manner of (FP), it is more convenient for computational reasons to integrate from  $\xi$  to infinity. Using the fact that

$$\int_0^\xi I_n d\xi = - \int_\xi^\infty I_n d\xi$$

and the simplification of the inelastic integrals used in (FP), we obtain the three equations

$$\xi^2 \theta F_0 + \xi(\alpha/\theta + \xi\theta) dF_0/d\xi + \phi(F_0(\xi)) = 0, \quad (9)$$

$$\xi^2 \theta F_1 + \xi \left( \frac{\alpha}{\theta} + \xi\theta \right) \frac{dF_1}{d\xi} + \phi(F_1(\xi)) + \frac{kT\alpha}{eE} \left[ \frac{\xi F_0}{\theta} - \int_{\xi}^{\infty} \frac{\xi}{\theta} \frac{dF_0}{d\xi} d\xi \right] - \frac{WM}{4NQ_0} \left( \frac{2}{mkT} \right)^{\frac{1}{2}} \int_{\xi}^{\infty} \xi^{1/2} F_0 d\xi = 0, \quad (10)$$

$$\begin{aligned} \xi^2 \theta F_2 + \xi \left( \frac{\alpha}{\theta} + \xi\theta \right) \frac{dF_2}{d\xi} + \phi(F_2(\xi)) + \frac{kT\alpha}{eE} \left[ \frac{\xi F_1}{\theta} - \int_{\xi}^{\infty} \frac{\xi}{\theta} \frac{dF_1}{d\xi} d\xi \right] - (M/4NQ_0)(2/mkT)^{1/2} \int_{\xi}^{\infty} (WF_1 - D_L F_0) \xi^{1/2} d\xi \\ - (kT/eE)^2 \alpha \int_{\xi}^{\infty} (\xi/\theta) F_0 d\xi = 0, \end{aligned} \quad (11)$$

where

$$\phi(F_n(\xi)) = \sum_j \int_{\xi}^{\xi + \xi_j} x \eta_j(x) F_n(x) dx - \exp(-\xi_j) \sum_j \int_{\xi - \xi_j}^{\xi} (x + \xi_j) \eta_j(x + \xi_j) F_n(x) dx.$$

In the manner of (FP) we then substitute  $F_0(\xi) = \gamma(\xi)V_0(\xi)$ ,  $F_1(\xi) = \gamma(\xi)V_1(\xi)$ , and  $F_2(\xi) = \gamma(\xi)V_2(\xi)$ , respectively, into Eqs. (9)–(11), where

$$\gamma(\xi) = \exp\left(-\int_0^{\xi} \{y\theta^2(y)/[\alpha + y\theta^2(y)]\} dy\right). \quad (12)$$

The equations then become

$$\xi(\alpha/\theta + \xi\theta)\gamma dV_0/d\xi + \phi(\gamma V_0) = 0, \quad (13)$$

$$\xi \left( \frac{\alpha}{\theta} + \xi\theta \right) \gamma \frac{d(NV_1)}{d\xi} + \phi(\gamma NV_1) + \frac{kT\alpha}{eE/N} \left[ \frac{\xi F_0}{\theta} - \int_{\xi}^{\infty} \frac{\xi}{\theta} \frac{dF_0}{d\xi} d\xi \right] - \frac{WM}{4Q_0} \left( \frac{2}{mkT} \right)^{\frac{1}{2}} \int_{\xi}^{\infty} \xi^{1/2} F_0 d\xi = 0, \quad (14)$$

$$\begin{aligned} \xi \left( \frac{\alpha}{\theta} + \xi\theta \right) \gamma \frac{d(N^2V_2)}{d\xi} + \phi(\gamma N^2V_2) + \frac{kT\alpha}{eE/N} \left[ \frac{\xi NF_1}{\theta} - \int_{\xi}^{\infty} \frac{\xi}{\theta} \frac{d(NF_1)}{d\xi} d\xi \right] \\ - (M/4Q_0)(2/mkT)^{1/2} \int_{\xi}^{\infty} (WNF_1 - ND_L F_0) \xi^{1/2} d\xi - (kTN/eE)^2 \alpha \int_{\xi}^{\infty} (\xi/\theta) F_0 d\xi = 0. \end{aligned} \quad (15)$$

From these equations it is seen that  $V_0$ ,  $NV_1$ , and  $N^2V_2$  or  $F_0$ ,  $NF_1$ , and  $N^2F_2$  are functions only of  $E/N$ .

The above equations enable  $D_L/\mu$  to be determined at any  $E/N$  and  $T$  provided that the momentum transfer cross section  $Q_m$ , which determines  $\theta$ , and the inelastic collision cross sections  $Q_{\pm j}$ , which determine  $\eta_{\pm j}$ , are known functions of energy. The procedure for evaluating  $D_L/\mu$  is to determine the following functions and quantities: (a)  $\gamma(\xi)$  from Eq. (12), (b)  $V_0(\xi)$  and thus  $F_0(\xi)$  from Eq. (13), (c)  $W$  and  $D_T/\mu$  from Eqs. (5) and (8), (d)  $NV_1(\xi)$  and thus  $NF_1(\xi)$  from Eq. (14), and (e)  $D_L/\mu$  from Eq. (7). To determine the magnitude of the higher-order correction terms, discussed in Sec. IV3, it is necessary to evaluate  $N^2V_2(\xi)$  and thus  $N^2F_2(\xi)$  from Eq. (15).

The evaluation of  $F_0$ ,  $F_1$ , and  $F_2$  from Eqs. (13)–(15) is not straightforward because of the integrals involving the unknown functions  $F_n$  in  $\phi(F_n(\xi))$ . For most calculations collisions of the second kind can be neglected and  $\phi$  is then simplified considerably. Thus, it is convenient to divide the calculations into two regimes; high  $E/N$ , where collisions of the second kind are neglected and low  $E/N$ , where collisions of the second kind are included.

### 1. High $E/N$

When collisions of the second kind are neglected, the energy gain terms expressed by the integrals  $\xi - \xi_j$  to  $\xi$  can be omitted. The function  $\phi$  is then given by

$$\phi(F_n(\xi)) = \sum_j \int_{\xi}^{\xi + \xi_j} x \eta_j(x) F_n(x) dx.$$

Equation (13), for example, is solved by using

the known property that  $F_0(\xi)$  tends to zero at high energy. One proceeds from a very high energy  $\delta$ , above which there are an insignificant number of electrons, and assumes that  $V_0(\xi) = 1$  for  $\xi \geq \delta$ . Then Eq. (13) is used to extend  $V_0(\xi)$  from  $\xi = \delta$  to  $\xi = 0$ . The function  $F_0(\xi)$ , obtained from  $F_0(\xi) = \gamma(\xi)V_0(\xi)$ , is then normalized using Eq. (6). When the inelastic term is zero,  $V_0(\xi) = 1$  and  $F_0(\xi) \propto \gamma(\xi)$ .

A difficulty arises in determining the functions  $V_1(\xi)$  and  $V_2(\xi)$  in that the boundary conditions<sup>1</sup>  $V_1(0)=0$  and  $V_2(0)=0$  have to be satisfied. The integration of Eqs. (14) and (15) cannot proceed from  $\xi=0$  because of the presence of integrals in the term representing inelastic collisions. However, the general solution of the integro-differential Eqs. (14) and (15) can be expressed as the sum of any particular integral and the complementary function. The homogeneous part of Eqs. (14) and (15) is simply Eq. (13) in terms of  $V_1$  and  $V_2$ . Consequently, the complementary function is  $V_0(\xi)$ . Equations (14) and (15) are solved in a similar way to Eq. (13), starting at a high energy  $\delta$ , letting  $V_1(\delta)$  and  $V_2(\delta)$  be a value which in principle is arbitrary, and integrating to zero energy. To these functions we then add  $c_n V_0(\xi)$ , where  $c_n$  is chosen to make  $V_n(0)=0$ .

In practice it is necessary to choose the starting values  $V_n(\delta)$ , to within a few orders of magnitude of the value which on integrating from  $\xi=\delta$  to  $\xi=0$  gives  $V_n(0)=0$ ; otherwise numerical errors result when adding the complementary function to satisfy the boundary conditions. From an analysis of the dominant terms in Eqs. (14) and (15), it is shown in the Appendix that at high energy  $F_1(\xi)$  and  $F_2(\xi)$  can be given approximately by

$$F_1(\xi) = -(2kT/eE)\xi F_0(\xi), \quad (16)$$

$$\text{and } F_2(\xi) = 2(kT\xi/eE)^2 F_0(\xi). \quad (17)$$

These expressions are used to provide starting values for  $V_n(\xi)$  at  $\xi \geq \delta$ .

## 2. Low $E/N$

Collisions of the second kind cannot be neglected at low  $E/N$ . In this case the procedure is again analogous to that of (FP). Equations (13)–(15) are each integrated from  $\xi$  to  $\delta$ . The integrals that are obtained involving  $V_n(\xi)$  are represented as summations involving a finite number of unknown quantities  $V_n(\xi_i)$ , where  $\xi_i$  ranges from 0 to  $\delta$ . A series of simultaneous linear equations in  $V_n(\xi_i)$  are then obtained which can be solved to obtain  $V_n(\xi_i)$  and thus the distribution function. It is again assumed that  $V_1(\xi)$  and  $V_2(\xi)$  for  $\xi \geq \delta$ , are determined by Eqs. (16) and (17). The boundary conditions  $V_1(0)=V_2(0)=0$  are again satisfied by use of the complementary function, as described previously. In practice computations for this low-energy region involve considerable computation time if high accuracy is required because computation time, at a minimum, increases at a rate proportional to the cube of the number of points taken to represent  $V_n(\xi)$ .

## IV. NUMERICAL RESULTS

### 1. Model Cross Sections

In I an example of the functions  $F_0(\epsilon)$ ,  $F_1(\epsilon)$ ,

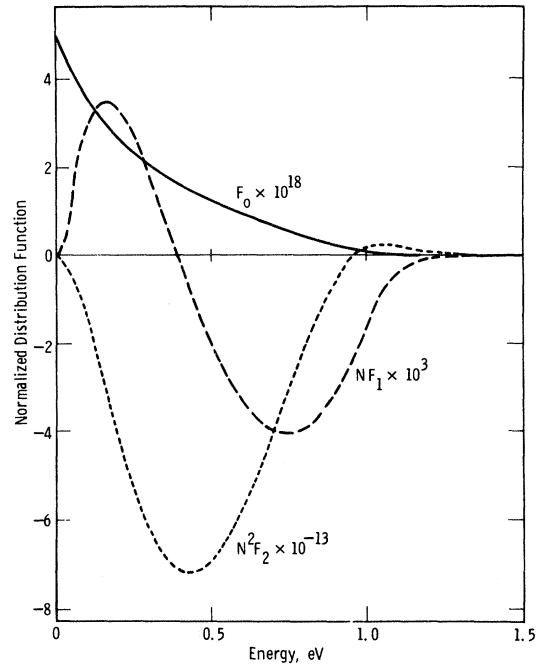


FIG. 1.  $F_0$ ,  $NF_1$ , and  $N^2F_2$  as a function of electron energy for the case of constant cross section and an inelastic energy-loss process of 1 eV. The units of  $F_0$ ,  $F_1$ , and  $F_2$  are  $\text{cm}^{-3}\text{sec}^3$ ,  $\text{cm}^{-2}\text{sec}^3$ , and  $\text{cm}^{-1}\text{sec}^3$ , respectively.

and  $F_2(\epsilon)$  was given for  $E/N=3 \times 10^{-17}$  at 77°K for the case of a collision cross section that was equal to  $6 \times 10^{-16} \text{ cm}^2$  and independent of energy. The molecular weight of the gas was taken to be 4. In Fig. 1 the functions  $F_0(\epsilon)$ ,  $F_1(\epsilon)$ , and  $F_2(\epsilon)$  are plotted for the same value of  $E/N$  for the case of constant momentum transfer cross section equal to  $6 \times 10^{-16} \text{ cm}^2$ , and in addition an inelastic cross section of magnitude  $10^{-16} \text{ cm}^2$  with a threshold of 1 eV and an energy loss for the inelastic process of 1 eV. The proportion of electrons at high energy, as indicated by  $F_0$ , is greatly reduced by the inelastic collisions. Also the form of  $F_1$  and  $F_2$  is changed and these functions, which indicate the dependence of the distribution function on position, are greatly reduced in magnitude.

The transport coefficients for these two cases are given in Table I.

The effect of inelastic collisions is to reduce the characteristic energy  $D_T/\mu$ , and also to reduce the variation of electron energy with position within a pulse. As a result, the ratio  $D_L/D_T$  changes from 0.5 in the purely elastic case to 0.9 with the addition of an inelastic process.

### 2. Longitudinal Diffusion

The results of the calculations of  $D_L/\mu$  for a number of real gases are presented in Figs.

TABLE I. Comparison of transport coefficient with and without inelastic collisions.

	$W$ (cm sec <sup>-1</sup> )	$D_T/\mu$ (V)	$D_L/\mu$ (V)
Elastic only	$9.11 \times 10^5$	1.42	0.700
Elastic + Inelastic	$20.4 \times 10^5$	0.288	0.258

2-8. Results are also shown for  $D_T/\mu$ , with which  $D_L/\mu$  is usually compared. The ratio  $D_L/D_T$  is unity at very low  $E/N$  where the electrons are in thermal equilibrium with the gas. At higher  $E/N$ , this ratio is dependent on the collision cross section, being particularly sensitive to the gradient of the momentum transfer cross section as a function of energy (see Table I in Paper I). The calculations of  $D_T/\mu$ , the results of which are presented in the figures, are a duplication of earlier calculations published in the references cited for each gas. In these investigations the collision cross sections were determined by obtaining consistency between calculated and experimental values of  $W$  and  $D_T/\mu$ . The experimental values of  $D_T/\mu$  shown in the figures were obtained by the Townsend method.<sup>5,6</sup> It is assumed that the experimental values can be identified with  $D_T/\mu$  as given by Eq. (8), and that the effects due to density gradients of electrons are negligible.<sup>7</sup> The experimental values of  $D_L/\mu$  are, in almost all cases, those of Wagner, Davis, and Hurst.<sup>8</sup> Their results were obtained from drift-tube measurements of the diffusion of electrons parallel to the electric field.

## (a) Helium

The input momentum transfer cross section for helium was that of Crompton, Elford, and Jory,<sup>9</sup> which was derived from measured values of the drift velocity. The derived values of  $D_T/\mu$  and magnetic drift velocity based on this cross section<sup>10</sup> agree with the experimental values of these quantities at 293°K to within the experimental errors of 1% and 2%, respectively, throughout the range of the measurements. Agreement between the experimental values of  $D_L/\mu$  and the theoretically derived values is thus a direct test of the present theory. There is no inelastic process for this case within the energy range of interest.

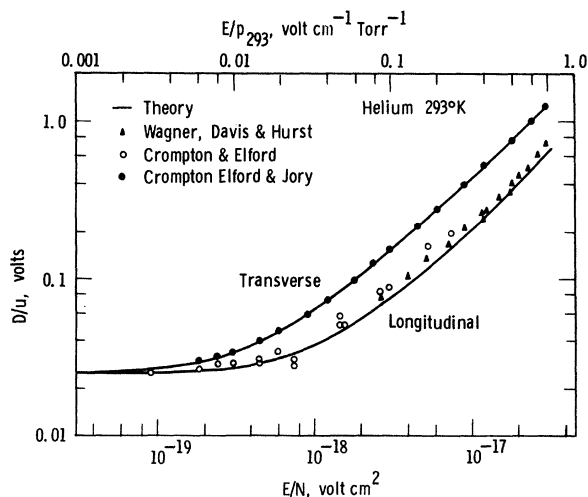
The experimental values of  $D_L/\mu$ , obtained by Wagner, Davis, and Hurst<sup>8</sup> are shown in Fig. 2 together with the theoretical predictions. The difference between experimental values of  $D_T/\mu$  and  $D_L/\mu$  is almost a factor of 2 for some values of  $E/N$ . Independent confirmation of this large difference between  $D_T/\mu$  and  $D_L/\mu$  has been ob-

tained by Crompton and Elford.<sup>11</sup> It is evident that the theory successfully explains the major part of the difference between  $D_T$  and  $D_L$ , but that the agreement between the experimental and theoretical values of  $D_L/\mu$  is by no means perfect, there being a remaining discrepancy of the order of 15%. More accurate measurements are desirable to determine whether a further extension of the theory is necessary.

## (b) Argon

By far the largest difference between  $D_T$  and  $D_L$  that has been reported<sup>8</sup> occurs in argon where the ratio  $D_L/D_T$  becomes as large as 7. Using the momentum transfer cross section derived by Engelhardt and Phelps,<sup>12,13</sup> the theory successfully explains this difference. The experimental and theoretical values of  $D_T/\mu$  and  $D_L/\mu$  are given for 77°K in Fig. 3. For  $E/N$  greater than  $2 \times 10^{-19}$ , the curves for  $D_T/\mu$  and  $D_L/\mu$  for 77°K are coincident with the curves for room temperature so that comparison with experimental data taken at room temperature is then valid. The experimental values of  $W$  and  $D_T/\mu$ , on which the momentum transfer cross section is based, are considerably less accurate than for the case of helium, and consequently the uncertainty in the momentum transfer cross section could account for the difference between the experimental and theoretical values of  $D_L/\mu$ .

Recent beam experiments of Golden<sup>14</sup> suggest that the Ramsauer minimum of the momentum transfer cross section may be much lower than that obtained by Engelhardt and Phelps.<sup>12</sup> However, derived values of the transport coefficients using the momentum transfer cross section of Golden give wider discrepancies with experi-

FIG. 2. Theoretical and experimental values of  $D_T/\mu$  and  $D_L/\mu$  for helium at 293°K.

mental transport coefficients than results obtained using the cross sections of Engelhardt and Phelps, as indicated in Fig. 3. Calculated values of  $D_L/\mu$  at  $E/N$  less than  $4 \times 10^{-20}$  cm<sup>2</sup> are seen to be particularly sensitive to the input cross section, and future experimental measurements in this region of  $E/N$  may enable the momentum transfer cross section to be determined more accurately.

(c) *Hydrogen and Deuterium*

In the molecular gases it is necessary to consider the effect of inelastic collisions due to rotational and vibrational excitation. Consequently further uncertainties in the input collision cross sections are introduced. However, using the H<sub>2</sub> cross sections obtained by Engelhardt and Phelps,<sup>15</sup> the derived values of  $D_L/\mu$  give very good agreement with the experimental values of Wagner, Davis, and Hurst.<sup>8</sup> For  $E/N$  such that  $D_T/\mu$  is less than 0.08 V, collisions of the second kind are considered and cross sections for four levels of rotational excitation were treated individually. For  $D_T/\mu$  greater than 0.08 V, the continuous approximation<sup>2</sup> for rotational excitation was used. The strength of the quadrupole moment was taken as  $0.56 ea_0^2$  ( $a_0$  is the Bohr radius) and a polarization correction factor<sup>15</sup> was included. The theoretical and experimental<sup>8,16</sup> values of  $D_T/\mu$  and  $D_L/\mu$  are given in Fig. 4.

Also shown in Fig. 4 are calculated values of  $D_L/\mu$  for deuterium. The input cross sections were those of Ref. 15 with seven levels of rota-

tional excitation being considered using a quadrupole moment of  $0.574 ea_0^2$ .

(d) *Nitrogen*

The input cross sections used for nitrogen were those of Engelhardt, Phelps, and Risk.<sup>17</sup> The equivalent quadrupole moment was taken as  $1.04 ea_0^2$ , and no polarization correction factor was used. For  $E/N > 2 \times 10^{-18}$  V cm<sup>2</sup>, the continuous approximation for rotational excitation was used and for  $E/N < 2 \times 10^{-18}$  V cm<sup>2</sup>, rotational cross sections were treated individually, 24 levels being considered. The theoretical and experimental values of  $D_L/\mu$  shown in Fig. 5 agree particularly well at low  $E/N$ .

(e) *Oxygen, Carbon Dioxide, and Water Vapor*

Experimental values of  $D_T/\mu$  are unavailable<sup>18</sup> at low  $E/N$  in oxygen because of the difficulty of making reliable measurements in the presence of electron attachment. As a consequence, the input cross sections, which are those of Hake and Phelps,<sup>19</sup> are of limited accuracy, particularly at low energy. The derived values of  $D_L/\mu$ , obtained using an equivalent quadrupole moment of  $1.8 ea_0^2$ , are given in Fig. 6. The single-level approximation<sup>19</sup> for rotational excitation was used for  $E/N < 6 \times 10^{-19}$  V cm<sup>2</sup>.

The theoretical values of  $D_L/\mu$  for carbon dioxide, based on the cross sections of Hake and Phelps,<sup>19</sup> are also given in Fig. 6. It is of interest that at low  $E/N$  the predicted ratio  $D_L/D_T$  is greater than unity because of the rapidly falling momentum transfer cross section. The only

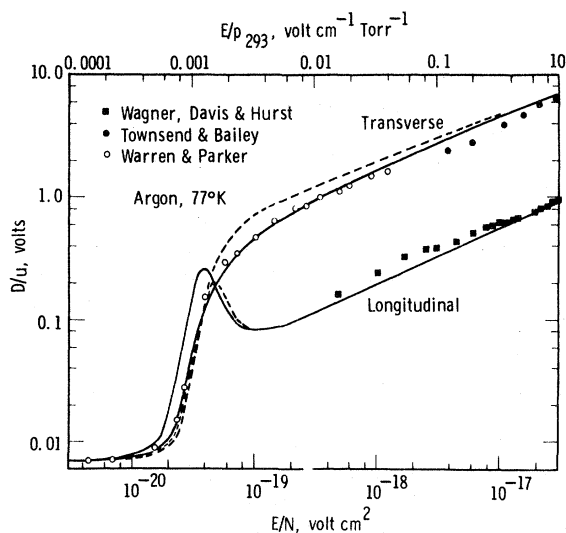


FIG. 3. Theoretical and experimental values of  $D_T/\mu$  and  $D_L/\mu$  for argon at 77°K. The full curve is obtained using as input the momentum transfer cross section of Engelhardt and Phelps, and the broken curve from using the momentum transfer cross section of Golden.

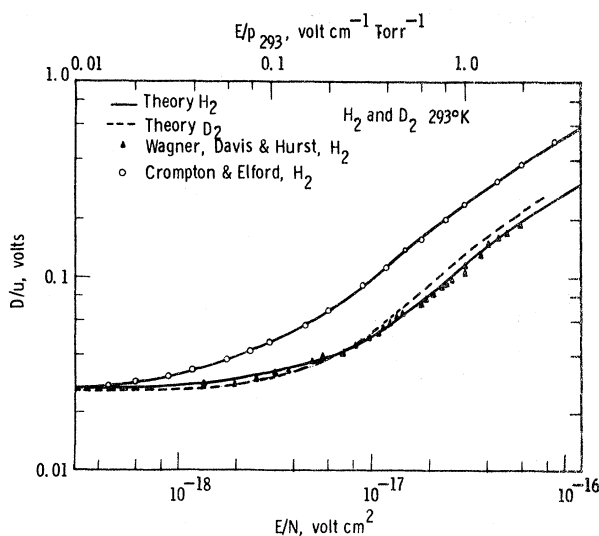


FIG. 4. Theoretical and experimental values of  $D_T/\mu$  and  $D_L/\mu$  for hydrogen at 293°K and theoretical values of  $D_L/\mu$  for deuterium at 293°K.

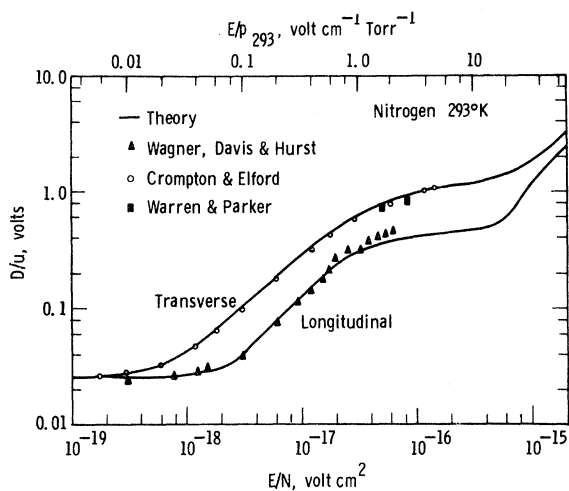


FIG. 5. Theoretical and experimental values of  $D_T/\mu$  and  $D_L/\mu$  for nitrogen at 293°K.

experimental measurements<sup>8</sup> of  $D_L/\mu$  are in a range of  $E/N$  for which it would be expected that the electron energy was thermal. Theoretical values of  $D_T/\mu$  for oxygen and carbon dioxide are given in Ref. 19.

The theoretical curves of  $D_T/\mu$  and  $D_L/\mu$  for water vapor are also shown in Fig. 6. The input cross sections are those of Cohen and Phelps,<sup>20</sup> the equivalent dipole moment being  $0.73 ea_0$ . As yet no experimental values of  $D_L/\mu$  exist, and furthermore the only reliable experimental values<sup>21</sup> of  $D_T/\mu$  are for  $E/N > 5 \times 10^{-16}$ . Consequently the input cross sections,<sup>20</sup> which are based on the available experimental values of  $W$  and  $D_T/\mu$ , must be regarded as being approximate.

The momentum transfer cross section for water

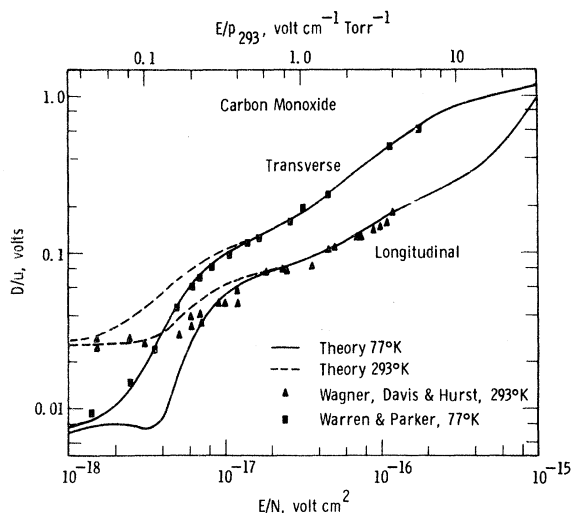


FIG. 7. Theoretical and experimental values of  $D_T/\mu$  and  $D_L/\mu$  for carbon monoxide at 77°K and 293°K.

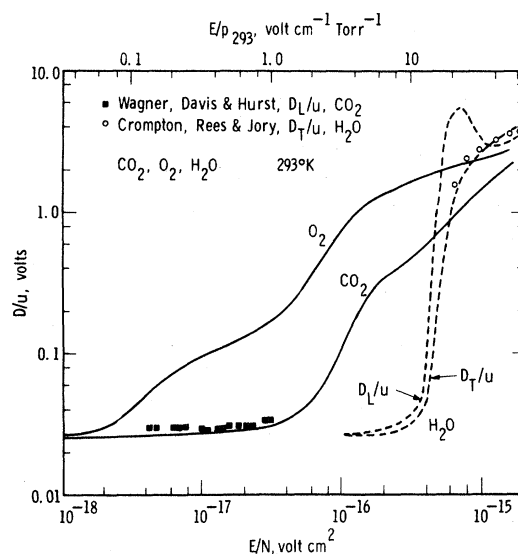


FIG. 6. Theoretical values of  $D_L/\mu$  for oxygen, carbon dioxide, and water vapor at 293°K. Also shown are experimental values of  $D_L/\mu$  for carbon dioxide and theoretical values of  $D_T/\mu$  for water vapor.

vapor is very large at low energy. Consequently water vapor has a strong thermalizing effect on electrons of low energy so that  $D_T \sim D_L$  until comparatively high values of  $E/N$  are reached. However, as the momentum transfer cross section falls initially<sup>22,23</sup> as  $1/\epsilon$ , the electron energy increases extremely rapidly as a function of  $E/N$  in this region and the theoretical values of  $D_L$  are greater than  $D_T$  by up to a factor of three.

#### (f) Carbon Monoxide

The theoretical values of  $D_T/\mu$  and  $D_L/\mu$  based on the cross sections of Hake and Phelps,<sup>19</sup> are compared with experimental results<sup>6,8</sup> in Fig. 7 for 77°K and 293°K. The continuous approximation for rotational excitation was used for all calculations, the value of the quadrupole moment being  $0.046 ea_0$ . At  $E/N$  as low as  $10^{-18}$  at 77°K, the continuous approximation gave<sup>19</sup> results for  $D_T/\mu$  equal to calculations using individual rotational cross sections to within 3%. However, at 293°K there is a considerable discrepancy between theoretical and experimental values of  $D_L/\mu$  in the region of  $E/N \sim 6 \times 10^{-18} \text{ V cm}^2$ . As the theoretical drift velocities at 293°K differ from experimental values by up to 7% in this region of  $E/N$ , it may be possible to adjust the input cross sections to give greater consistency.

#### (g) Krypton and Xenon

Calculated values of  $D_L/\mu$  for krypton and xenon, based on the cross sections of Frost and Phelps,<sup>13</sup> are shown in Fig. 8. Values of  $D_T/\mu$ ,

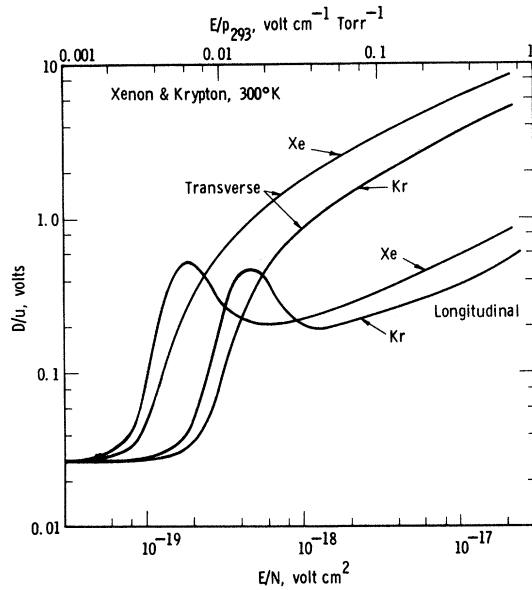


FIG. 8. Theoretical values of  $D_T/\mu$  and  $D_L/\mu$  for krypton and xenon at 300°K.

previously calculated by Frost and Phelps,<sup>13</sup> but not published, are also given in this figure. There are no published experimental values of  $D_L/\mu$  for these gases.

### 3. Calculation of Higher-Order Terms

The terms involving  $A_1$  and  $A_2$  in Eqs. (33) and (34) of Paper I have also been evaluated, using Eq. (32) of I, i. e.,

$$A_i = (4\pi kT/m)(2kT/m)^{1/2} \int_0^\infty \xi^{1/2} F_i d\xi. \quad (18)$$

These terms describe departures of the drift and diffusion of a pulse from that represented by  $W$  and  $D_L/\mu$ . The effect of these terms can be represented by a multiplying factor, e. g., for Eq. (34) of I

$$D_{Lp}/\mu = (1 + cD_T/Wz_{av})D_L/\mu,$$

where  $D_{Lp}$  is defined by  $2D_{Lp}t = (z - z_{av})z_{av}^2$ ;  $z_{av}$  is the drift distance and  $c$  is a dimensionless constant independent of pressure given by  $c = (A_2 - A_1^2/2)(W/D_T)^2$ . The same correction factor<sup>24</sup> can be obtained from Eq. (33) of I, but with  $c = -A_1W/D_T$ .

It is to be noted that the correction is small when the energy relaxation distance  $D_T/W$ , as discussed in I, is small in comparison to the drift distance. The value of  $c$ , for all gases<sup>25</sup> except water vapor, for both the drift velocity and the  $D_L/\mu$  correction was less than 3 for all values of  $E/N$  that were investigated. It is stressed that the values of  $c$  that have been cal-

culated apply only for a pulse whose electrons are initially at zero energy. While derived values of  $c$  cannot be used to make quantitative corrections to experimental measurements unless account is taken of the initial energy distribution, they do indicate the order of magnitude of these corrections. For usual experimental conditions the correction is less than 10%. For example, in hydrogen  $c = 1$  corresponds to a correction of 1% at a pressure of 10 Torr for  $E/p = 0.1$  V cm<sup>-1</sup> Torr<sup>-1</sup> and a drift distance of 5 cm. Even in water vapor, where the value of  $c$  is calculated to be approximately 100 at  $E/N = 4 \times 10^{-16}$  V cm<sup>2</sup>, the correction is only 8% for a pressure of 1 Torr and a drift distance of 5 cm.

### V. ACCURACY OF NUMERICAL RESULTS FOR $D_L/\mu$

The accuracy of the calculations of  $D_L/\mu$  is generally 2%. However, in exceptional cases, for example, in water vapor where the cross section falls rapidly with energy, the numerical errors could be as large as 10% in the range of  $E/N$  where electron energy is changing very rapidly with  $E/N$ . The numerical accuracy was assessed by halving the integration step size, and comparing the values of  $D_L/\mu$ .

Further checks on the numerical accuracy of the  $D_L/\mu$  calculations are as follows:

(a) For the case of "constant collision frequency," i. e.,  $\theta \propto 1/\epsilon^{1/2}$  it can be shown analytically<sup>1</sup> that  $D_T = D_L$ . The numerical results of  $D_T$  and  $D_L$  for  $\theta \propto 1/\epsilon^{1/2}$  agree to within 2%.

(b) It can be shown analytically that  $D_L/\mu$  is unchanged if  $F_1(\xi) + cF_0(\xi)$  is substituted for  $F_1(\xi)$ , where  $c$  is any constant. This result follows from Eq. (7) because, using Eqs. (5) and (6)

$$\frac{1}{3} \left( \frac{2}{mkT} \right)^{1/2} \frac{e}{Q_0 W} \left( \frac{E}{N} \right)^2 \int_0^\infty \frac{\xi}{\theta} \frac{dNF_0}{d\xi} d\xi + (E/N) \int_0^\infty \xi^{1/2} NF_0 d\xi = 0.$$

Thus, derived values of  $D_L/\mu$  should be independent of whether or not a complementary function  $cF_0(\xi)$  is added to the particular integral to make the solution  $F_1(\xi)$  pass through the origin, and this property has been used to test the computation program.

### VI. SUMMARY

Using a theoretical analysis of electron diffusion described previously,<sup>1</sup> numerical values of the diffusion coefficient parallel to the electric field have been derived as a function of  $E/N$  for the common gases. Differences exist between the longitudinal and transverse diffusion coefficients

of the order of a factor of seven in argon and a factor of two in helium, hydrogen, and nitrogen, which is in agreement with experimental observations.<sup>8</sup> Differences of the order of 15% between theoretical predictions and experimental observations still exist, and further investigation is required to determine whether these differences are due to experimental inaccuracies, incorrect input cross sections or whether a still more refined theoretical treatment is required.

It has also been shown that providing that the drift distance is large compared with the relaxation distance, the departures of the electron pulse shape from that of a Gaussian traveling at speed  $W$  and characterized by a diffusion coefficient  $D_L$ , are small.

#### ACKNOWLEDGMENTS

The authors are particularly indebted to A. V. Phelps for numerous helpful discussions. We also thank R. W. Crompton and M. T. Elford for making available their experimental measurements of  $D_L/\mu$  in helium.

#### APPENDIX: BEHAVIOR OF $F_1(\xi)$ AND $F_2(\xi)$ AT HIGH ENERGY

In Eqs. (3) and (4) we retain only the terms which dominate at high energy to obtain, where  $n=1$  or 2,

$$\begin{aligned} & (d/d\xi)[\xi^2\theta F_n(\xi) + \xi(\alpha/\theta)dF_n(\xi)/d\xi] \\ & + I_n + (2kT\alpha/eE)(d/d\xi)[\xi F_{n-1}(\xi)/\theta] = 0 \quad (A1) \end{aligned}$$

If  $I_n$  can be expressed as  $d/d\xi[\eta(\xi)g(\xi)F_n(\xi)]$ , [for the continuous approximation for rotational excitation of (FP)  $g(\xi)=\xi$ ], Eq. (A1) can be integrated to yield

$$\frac{dF_n}{d\xi} + h(\xi)F_n = -\frac{2kT}{eE}F_{n-1}, \quad n=1 \text{ or } 2, \quad (A2)$$

where  $h$  is a function of  $\xi$ . The constant of integration from the integration of (A1) is zero as  $F_n \rightarrow 0$  as  $\xi \rightarrow \infty$ . The solution of the homogeneous part of (A2), as for Eqs. (10) and (11), is  $F_0$ , i.e., at high energy  $F_0$  is given by

$$F_0(\xi) = \exp[-\int_0^\xi h(y)dy].$$

On solving Eq. (A2) we obtain

$$\begin{aligned} F_n(\xi) = & -\exp[-\int_0^\xi h(y)dy] \\ & \times (2kT/eE) \int_0^\xi \exp[\int_0^x h(y)dy] F_{n-1}(x) dx. \end{aligned}$$

Thus for  $n=1$  we obtain

$$F_1(\xi) = -(2kT/eE)\xi F_0(\xi), \quad (A3)$$

and for  $n=2$ ,

$$F_2(\xi) = -F_0(\xi) \frac{2kT}{eE} \int_0^\xi \frac{F_1(z)}{F_0(z)} dz = 2 \left( \frac{kT\xi}{eE} \right)^2 F_0(\xi). \quad (A4)$$

Note that these approximations are valid at high energy regardless of whether elastic or inelastic collisions are dominant at high energy.

The authors are indebted to A. V. Phelps for suggesting the procedure of this Appendix.

<sup>1</sup>J. H. Parker, Jr. and J. J. Lowke, Phys. Rev. **181**, 290 (1969).

<sup>2</sup>L. S. Frost and A. V. Phelps, Phys. Rev. **127**, 1621 (1962).

<sup>3</sup>T. Holstein, Phys. Rev. **70**, 367 (1946).

<sup>4</sup>This normalization differs from that used in Ref. 2.

<sup>5</sup>L. G. H. Huxley and R. W. Crompton in, Atomic and Molecular Processes, edited by D. R. Bates (Academic Press, Inc., New York, 1962), Chap. 10.

<sup>6</sup>R. W. Warren and J. H. Parker, Jr., Phys. Rev. **128**, 2661 (1962).

<sup>7</sup>An analysis of the effect of density gradients in Townsend experiments has been given previously.

James H. Parker, Jr., Phys. Rev. **132**, 2096 (1963).

<sup>8</sup>E. B. Wagner, F. J. Davis, and G. S. Hurst, J. Chem. Phys. **47**, 3138 (1967). See also G. S. Hurst and J. E. Parks, J. Chem. Phys. **45**, 282 (1966).

<sup>9</sup>R. W. Crompton, M. T. Elford, and R. L. Jory, Australian J. Phys. **20**, 369 (1967). Earlier cross sections in helium based on swarm experiments were given by L. S. Frost and A. V. Phelps, Phys. Rev. **136**,

A1538 (1964).

<sup>10</sup>Theoretical cross sections derived by J. Callaway, R. W. LaBahn, R. T. Pu, and W. M. Duxler, Phys. Rev. **168**, 12 (1968) agree to 6% with the momentum transfer cross section of Ref. 9.

<sup>11</sup>R. W. Crompton and M. T. Elford, private communication. Further evidence that  $D_L$  is much lower than  $D_T$  in helium is provided by the oscillographic current pulses given by J. C. Bowe, Phys. Rev. **117**, 1411 (1960). These pulses decrease more rapidly than would be predicted using the appropriate known value of  $D_T/\mu$ .

<sup>12</sup>A. G. Engelhardt and A. V. Phelps, Phys. Rev. **133**, A375 (1964).

<sup>13</sup>L. S. Frost and A. V. Phelps, Phys. Rev. **136**, A1538 (1964).

<sup>14</sup>D. E. Golden, Phys. Rev. **151**, 48 (1966).

<sup>15</sup>A. G. Engelhardt and A. V. Phelps, Phys. Rev. **131**, 2115 (1963).

<sup>16</sup>R. W. Crompton and M. T. Elford, Proceedings of the Sixth International Conference on Ionization Phenomena in Gases, Paris, 1963, edited by P. Hubert and

E. Crémieu-Alcan (European Atomic Energy Community, 1964), Vol. 1, p. 337.

<sup>17</sup>A. G. Engelhardt, A. V. Phelps, and C. G. Risk, Phys. Rev. **135**, A1566 (1964).

<sup>18</sup>It should be possible to obtain experimental values of  $D_L/\mu$  over almost the same range of  $E/N$  for which measurements have been made for  $W$ . The ability to distinguish electrons of a current pulse in a drift-tube experiment from current due to attached electrons may enable measurements of  $D_L/\mu$  to be made with greater ease than  $D_T/\mu$  in the region of  $E/N$  where electron attachment is significant.

<sup>19</sup>R. D. Hake, Jr. and A. V. Phelps, Phys. Rev. **158**, 70 (1967).

<sup>20</sup>R. Cohen and A. V. Phelps, Westinghouse Research Laboratories, Pittsburgh, 1968 (unpublished).

<sup>21</sup>R. W. Crompton, J. A. Rees, and R. L. Jory, Australian J. Phys. **18**, 541 (1965).

<sup>22</sup>J. L. Pack, R. E. Voshall, and A. V. Phelps, Phys. Rev. **127**, 2084 (1962).

<sup>23</sup>K. Takayanagi, J. Phys. Soc. (Kyoto) **21**, 507 (1966).

<sup>24</sup>In a conventional analysis of the effect of boundary conditions imposed by the electrodes, (J. J. Lowke, Australian J. Phys. **15**, 39 (1962)), the same factor  $1 + c D_T/Wz_{av}$  was obtained for pressure dependent corrections in drift velocity experiments. The value of  $c$  in this case was approximately 3 to 5. A more detailed analysis of D. S. Burch predicts  $c$  to be approximately zero (private communication).

<sup>25</sup>Tabulated values of  $c$ , and also values of  $D_T/\mu$ ,  $D_L/\mu$ , and  $W$  are given as a function of  $E/N$  in Westinghouse Scientific Paper No. 68-1E0-GASES-P8.

## Velocity-Dependent Orbitals in Proton-On-Hydrogen-Atom Collisions\*

S. B. Schneiderman†

*United Aircraft Research Laboratories, East Hartford, Connecticut 06108*

and

A. Russek

*Physics Department, The University of Connecticut, Storrs, Connecticut 06268*

(Received 15 January 1969)

Requirements are outlined for a suitable set of dynamic orbitals for theoretical studies in collision problems. The effect of these upon the wave function, dynamic energy correction, and effective internuclear potential are all considered. It is shown that earlier forms suggested for this type of problem do not meet all required dynamic boundary conditions, principally because of their failure to recognize that physically, for moderate speed collisions, the electron at times "belongs" to the "molecule" proper and not to either atom individually. The earlier orbitals also fail to make allowances for the reluctance of an electronic charge distribution to follow rapid rotation of an internuclear axis. These considerations suggest a new form of dynamic orbital which by remedying these deficiencies automatically achieves complete orthonormality. The results of preliminary charge transfer calculations with the new orbital basis are presented.

### I. INTRODUCTION

There have been many attempts,<sup>1,2</sup> recently some notably successful ones,<sup>3,4</sup> at a theoretical verification of the remarkable differential cross-section data of Everhart *et al.*<sup>5</sup> for charge exchange in the proton-on-hydrogen-atom system. One result of all these efforts has been the emergence of two clear shortcomings of the original method of perturbed stationary states (pss) proposed by Bates, Massey, and Stewart.<sup>6</sup> These are (1) failure of the theory to account, in charge transfer processes, for transfer of the momentum of the electron and

(2) failure of the theory to account for the reluctance of electronic eigenfunctions to follow the rotation of an internuclear line in even moderate speed collisions. Both of these failures are due to the inability of the theory to account for velocity-dependent effects caused by the presumably small, yet finite, relative velocity of the colliding particles and both enter into the mathematics of the theory through the form chosen for the electronic basis functions. Bates and McCarroll<sup>7</sup> showed that the first of the above difficulties was related to the inability of an adiabatic basis to match the correct asymptotic form for the system wave function and